Cancer Letters 442 (2019) 252–261

Contents lists available at ScienceDirect

Cancer Letters

journal homepage: www.elsevier.com/locate/canlet

Original Articles

# YTHDF2 suppresses cell proliferation and growth via destabilizing the EGFR mRNA in hepatocellular carcinoma

Li Zhong[a,1], Dan Liao[a,1], Meifang Zhang[a], Cuiling Zeng[a], Xinchun Li[a], Ruhua Zhang[a], Haiqing Ma[b,*], Tiebang Kang[a,*]

[a] State Key Laboratory of Oncology in South China, Collaborative Innovation Center for Cancer Medicine, Sun Yat-sen University Cancer Center, Guangzhou, China
[b] Department of Oncology, The Fifth Affiliated Hospital of Sun Yat-Sen University, Zhuhai, Guangdong, China

ARTICLE INFO

*Keywords:*
YTHDF2
EGFR
mRNA
ERK
HCC

ABSTRACT

$N^6$-methyladenosin ($m^6A$) is one of the most pervasive modification of mRNA in eukaryotes and the $m^6A$ methyltransferases and demethylases play critical roles in many types of cancer. However the role of $m^6A$-binding proteins in cancer remains elusive. Here we report that the down-regulation of YTHDF2 was specifically induced by hypoxia in hepatocellular carcinoma (HCC) cells, and that overexpression of YTHDF2 suppressed cell proliferation, tumor growth and activation of MEK and ERK in HCC cells. Mechanistically, YTHDF2 directly bound the $m^6A$ modification site of EGFR 3'-UTR to promote the degradation of EGFR mRNA in HCC cells. This is the first report showing that YTHDF2 may act as a tumor suppressor to repress cell proliferation and growth via destabilizing the EGFR mRNA in HCC.

## 1. Introduction

Hepatocellular carcinoma (HCC) is the predominant form of liver cancer, which ranks the second cancer related mortality worldwide with more than 700,000 annual deaths globally in recent year [1]. Despite resection, liver transplantation or local ablation contribute to curative therapies in early stage of HCC [2], the prognosis of HCC is still poor due to the late diagnosis or advanced liver cirrhosis. Therefore, it is urgent to understand molecular mechanism of HCC initiation and progression.

$N^6$-methyladenosin($m^6A$) as one of the most pervasive modification of mRNA in eukaryotes has been reported to be functional in many biological processes, such as mRNA stability [3], protein translation [4], virus infection [5] and embryonic development [6]. Recently emerging evidences show that dysregulation of $m^6A$ modification and $m^6A$ associated proteins may play a critical role in initiation and progression of cancer [7]. For instance, METTL14 (Methyltransferase Like 14) and METTL3 (Methyltransferase Like 3) as the $m^6A$ methyltransferases are highly expressed in AMLs (Acute Myeloid Leukemia) and promote leukemogenesis through $m^6A$-dependent regulation of their target mRNAs [8,9]. FTO (Fat-Mass and Obesity-Associated Protein) as a $m^6A$ demethylase is highly expressed in AMLs and plays oncogenic roles in AMLs [10]. ALKBH5 (α-Ketoglutarate-Dependent Dioxygenase AlkB Homolog 5), another $m^6A$ demethylase, maintains the self-renewal of glioblastoma and breast cancer stem cells through regulating its target genes FOXM1 (Forkhead Box M1) [11] and NANOG (Nanog Homeobox) [12], respectively.

The fates of $m^6A$ modified mRNAs are dependent on $m^6A$ selective binding proteins [13]. YTHDF2 (YTH-Domain Family Member 2) is the first identified and well-studied functional $m^6A$-binding protein that mainly regulates stability of mRNA [3]. YTHDF2 recognizes and binds to $m^6A$ sites in 3'UTR of mRNA through its C-terminal YTH (YT521-B Homology) domain [14,15] and recruits the CCR4 (carbon catabolite repressor protein 4)-NOT (negative on TATA) deadenylase complex by directly binding CNOT1 (CCR4-NOT transcription complex subunit 1) via its N-terminal region to accelerate degradation of target mRNAs [16]. It has been reported that YTHDF2 has dual roles in pancreatic cancer cells by promoting proliferation and suppressing migration and invasion [17]. However, the role of YTHDF2 in HCC remains to be explored. In the present study, we demonstrated that YTHDF2 may act as a tumor suppressor by promoting the degradation of EGFR mRNA in HCC.

* Corresponding authors.
*E-mail addresses:* mahaiqing@mail.sysu.edu.cn (H. Ma), kangtb@mail.sysu.edu.cn (T. Kang).
[1] These authors contributed equally to this work.

https://doi.org/10.1016/j.canlet.2018.11.006
Received 4 September 2018; Received in revised form 25 October 2018; Accepted 5 November 2018

## 2. Materials and method

### 2.1. Cell culture

Four cell lines (QGY7703, BEL7402, HEP3B and SMMC7721) were kindly provided by Prof. Zheng [18]. QGY7703 and BEL7402 cells were cultured in DMEM (Gibco, USA). HEP3B and SMMC7721 cells were cultured in RPMI-1640 medium (Gibco, USA). HEK-293T was purchased from the American Type Culture Collection (ATCC) and maintained in DMEM (Gibco, USA). All culture medium supplemented with 10% (vol/vol) fetal bovine serum (FBS) (Gibco, USA), 1%(vol/vol) penicillin and streptomycin (Beyotime Biotech, China). All cell lines used in this research were authenticated by using short-tandem repeat profiling less than 6 months ago when this project was initiated and were cultured no more than 2 months. For hypoxia treatment, cells were placed into an incubator chamber containing 1% of $O_2$, 5% of $CO_2$ and 94% of $N_2$ or treated with Cobalt(II) chloride (sigma) for the indicated time.

### 2.2. Plasmid construction

The flag-tagged N-YTHDF2 (1–384 amino acids), C-YTHDF2 (385–579 amino acids) and YTHDF2 (1–579 amino acids) were amplified by PCR and cloned into PSIN-EF2-Puro lenti-viral vector (Invitrogen). The YTHDF2-2A-Mut (K416A, R527A), YTHDF2-3A-Mut (W432A, W486A, W491A) and YTHDF2-5A-Mut (K416A, W432A, W486A, W491A, R527A) mutants were conducted by Mut Express® II Fast Mutagenesis Kit (Vazyme) and verified by DNA sequencing. The pmirGlo luciferase expression vector (Promega) was used to construct the luciferase reporter plasmid that consists of both firefly luciferase and renilla luciferase. The 3'UTR region of EGFR mRNA was inserted after the F-luc coding sequence. The mutant EGFR luciferase reporter plasmid was constructed by replacing the adenosine to cytosine of $m^6A$ modification sites. The PLKO.1-puro vector (Sigma) was used to construct shRNAs targeting YTHDF2 or CNOT1. The lenti-CRISPR vector (Addgene) was used to clone the sgRNAs targeting YTHDF2. The sequences of shRNAs and sgRNAs are shown in Supplementary Materials.

### 2.3. qRT-PCR

Briefly, Total RNA was isolated by using Trizol reagent (Invitrogen, USA). 500 ng total RNA was reversed transcribed by using HiScript II 1st Strand cDNA Synthesis Kit (Vazyme). qRT-PCR was performed using ChamQ Universal SYBR qPCR Master Mix (Vazyme) and LightCycler 480 instrument according to the manufacturer's instructions. All reactions were conducted at least three replication. The sequences of primers are shown in Supplementary Materials.

### 2.4. Western blotting and antibodies

Briefly, Whole cell lysates were prepared and subjected to be separated by SDS–polyacrylamide gel electrophoresis and transferred onto polyvinylidene difluoride membranes. The membranes were blocked with 5% non-fat milk for 1 h at room temperature and incubated with primary antibodies and HRP-conjugated secondary antibody. The chemiluminescent signaling was detected by using ECL reagents (Pierce, USA). Primary antibodies used in this study: anti-YTHDF2 (24744-1-AP) was from proteintech, anti-HIF1α (610958) was from BD Bioscience, anti-Flag(2368), anti-ERK (4695), anti-MEK (8727), anti-AKT (4691), anti-p-ERK (4370), anti-p-MEK (2338) and anti-p-AKT (4060) were from cell signaling technology.

### 2.5. Immunofluorescence

Cells were seed into confocal dish (NEST) and fixed with 4% paraformaldehyde for 10 min at room temperature. After permeabilization with 0.5% Triton X-100 for 10 min, cells were blocked with 5% goat serum and incubated with primary antibody overnight at 4 °C. The next day, cells were washed and incubated with secondary antibody at room temperature for 1 h. And then were labeled the nuclei by using Hoechst 33342 for 5 min.

### 2.6. Luciferase reporter assay

Briefly, HCC cells were plated in the 24-well plate and then were transiently transfected with 250 ng 3'UTR luciferase reporter plasmid (Promega E1330). The luciferase activity was measured for at least three independent experiments by using a Dual-Luciferase Assay kit (Promega) after transfection for 48 h.

### 2.7. Clonogenic assay

HCC stable cells were seeded at the density of 500 per well in 6-well plates. After 2 weeks, the cell clones were fixed in methanol and stained with 0.1% crystal violet. Cell clones containing more than 50 cells were counted.

### 2.8. Anchorage-independent growth assay

HCC stable cells were resuspended in 2 ml 0.3% agarose at the density of $1 \times 10^4$ and were plated in 6 well plates with 0.6% agarose. Cells were cultured for 2 weeks and the foci formation containing more 50 cells were counted.

### 2.9. Cell viability assay

HCC stable cells were seeded in 96-well microplate at the density of 2500 cells per well and 3-(4, 5-Dimethylthiazol-2-yl)-2, 5-diphenyltetrazolium bromide (MTT) assay was used to assess cell viability per day for continuous five days.

### 2.10. Flow cytometric apoptosis assay

HEP3B, QGY7703, SMMC7721 and BEL7402 stable cells were treated with Cisplatin (DDP) 10 μM for 48 h and were collected. Annexin V- FITC-PI Apoptosis Detection Kit (KeyGEN) was used to stain the harvested stable cells, and then were analyzed using Gallios Flow Cytometer (Beckman Coulter).

### 2.11. Tumor xenograft model

Animal studies were approved by the Animal Research Committee of Sun Yat-sen University Cancer Center. Male athymic BALB/C nude mice (4 weeks old) were obtained from the Vital River Laboratory Animal Technology (Beijing, China). Briefly, $5 \times 10^6$ of HEP3B and SMMC7721 stable cells were resuspended in 0.1 ml of PBS and subcutaneously injected into the flank of mice. The right flank was inoculated with HCC cells stably expressing YTHDF2 and the left flank was inoculated with vector HCC cells. Tumor size was measured twice a week and calculated by the formula: $\text{width}^2 \times \text{length} \times \pi/6$. All mice were sacrificed after 4 weeks and xenograft tumor burdens were isolated, photographed, weighed and fixed in formalin.

### 2.12. Measurement of EGFR mRNA stability

Stable cells were incubated with actinomycin D for 0 h, 3 h or 6 h and then followed by RNA extraction. And the half-life of EGFR mRNA was analyzed by quantitative RT-PCR as described earlier [19].

### 2.13. Statistical analysis

Results are presented as mean ± SD for at least three independent

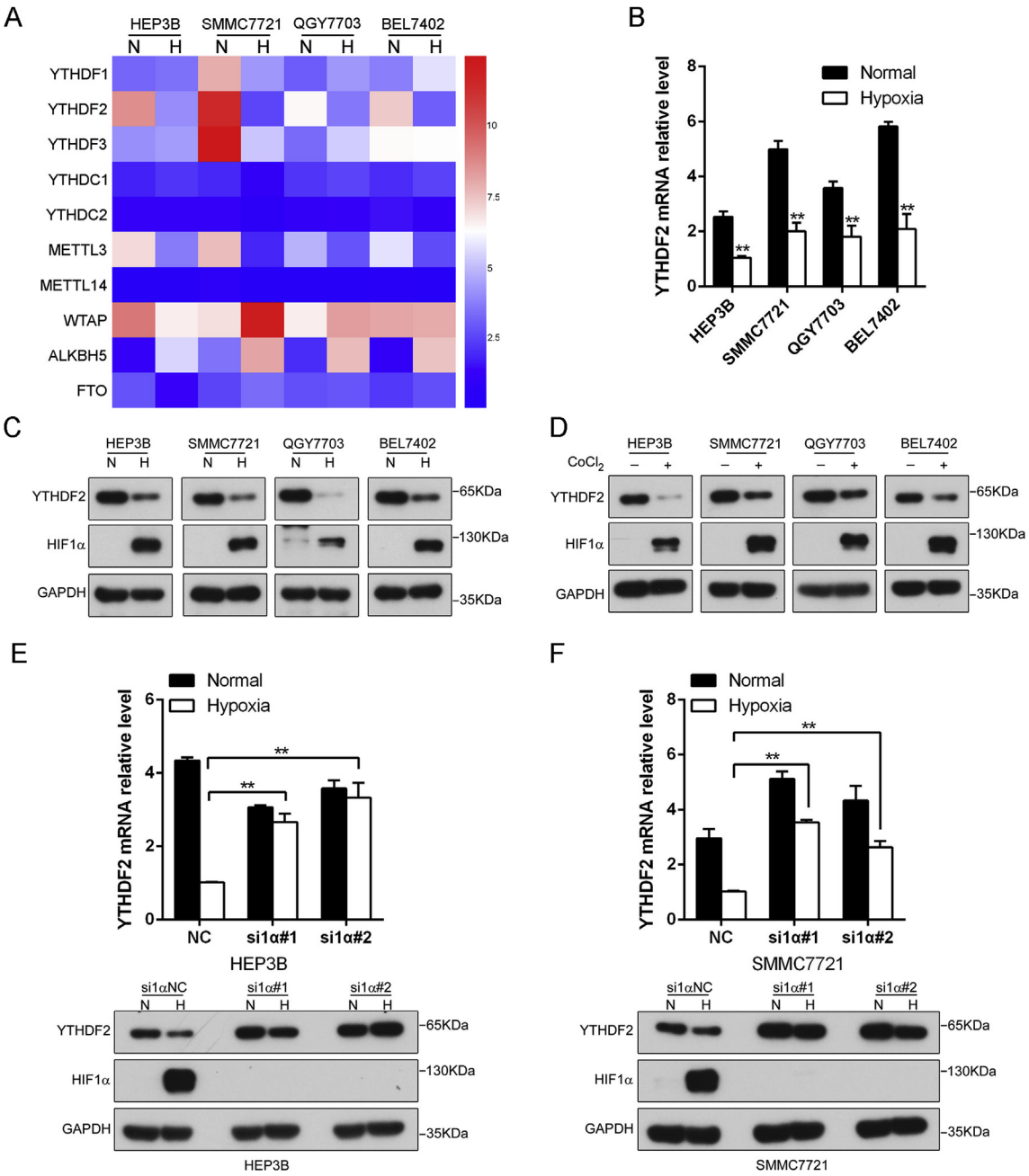


**Fig. 1.** Down-regulation of YTHDF2 under hypoxia in HCC cells. (**A**) The indicated HCC cells were exposed to 20% $O_2$ or 1% $O_2$ for 24 h, and differential expression patterns of the $m^6A$ methyltransferases (METTL3, METTL14, WTAP), the $m^6A$ demethylases (ALKBH5, FTO) and the $m^6A$ -binding protein (YTHDF1, YTHDF2, YTHDF3, YTHDC1, YTHDC2) were presented by a heat map. (**B**) The indicated HCC cells were cultured under 20% $O_2$ or 1% $O_2$ for 24 h, and mRNA levels of YTHDF2 were analyzed by RT-qPCR (mean ± SD. n = 3. Student *t*-test. $^{**}p < 0.01$). (**C**) Both YTHDF2 and HIF1α protein levels were determined by Western blotting in the indicated HCC cells under hypoxia or normoxia condition. GAPDH was used as the loading control (n = 3). (**D**) The indicated stable cells were treated with $CoCl_2$ or vehicle for 24 h and were analyzed by Western blotting. GAPDH was used as the loading control (n = 3). (**E** and **F**) The indicated stable cells were transfected with siRNA targeting HIF1α for 6 h and then were cultured under 20% $O_2$ or 1% $O_2$ for 24 h. YTHDF2 mRNA and protein levels were determined by RT-qPCR and Western blotting, respectively (mean ± SD. n = 3. two way ANOVA with Bonferroni test. $^{**}p < 0.01$).

experiments. Student's t-test was used to analyze difference between two groups and ANOVA with the Bonferroni *post hoc* test was used to analyze difference among multiple groups.$^{*}P < 0.05$ and $^{**}P < 0.01$ was considered significant.

## 3. Results

### 3.1. YTHDF2 was specifically down-regulated by hypoxia in HCC cells

Hypoxia is a common feature of many solid cancers including HCC, and promotes angiogenesis, self-renewal of cancer stem cells, tumor progression and chemotherapy resistance through gene regulation by hypoxia-inducible factor (HIF) [20]. Using four HCC cell lines, SMMC7721, HEP3B, BEL7402 and QGY7703, we tried to investigate whether the $m^6A$ associated proteins, including the $m^6A$-binding proteins (YTHDF1, YTHDF2, YTHDF3, YTHDC1 and YTHDC2), the $m^6A$ methyltransferases (METTL3, METTL14 and WTAP) and the $m^6A$ demethylases (ALKBH5 and FTO), are affected by hypoxia. As shown in Fig. 1A, among the five $m^6A$ binding proteins, YTHDF2 as the core component of the $m^6A$-binding protein was the only one that was

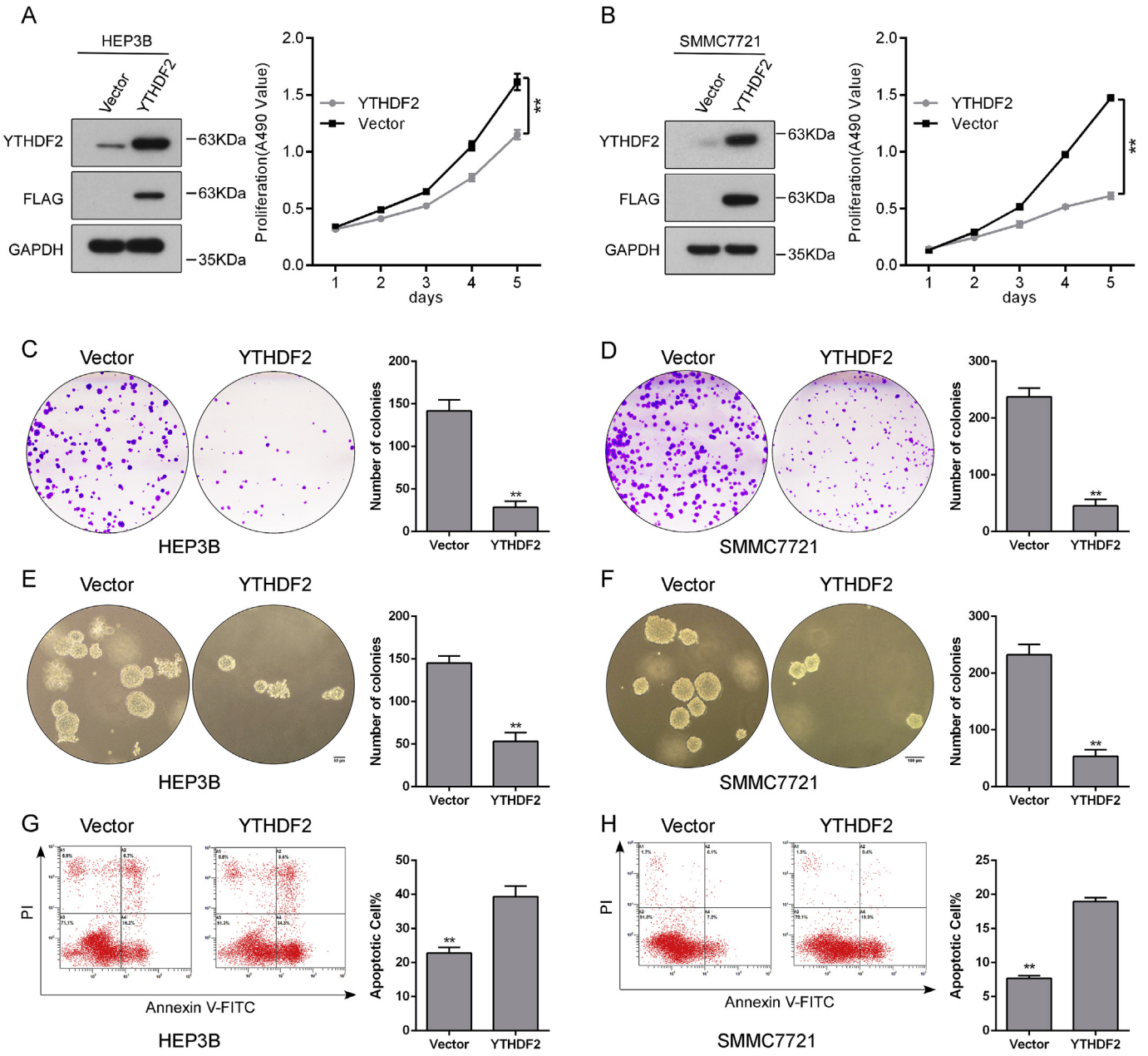


**Fig. 2.** Overexpression of YTHDF2 suppresses cell proliferation and growth, and promotes apoptosis in HCC cells. (**A** and **B**) The indicated stable cells were subjected to Western blotting (Left panel) and the MTT assay (Right panel). The cell viability was measured by MTT assay at different time points (mean ± SD. n = 3. Student *t*-test. $^{**}p < 0.01$). (**C** and **D**) Colony-formation assay of the indicated stable cells. The quantitative analysis was shown adjacent to representative images (mean ± SD. n = 3. Student *t*-test. $^{**}p < 0.01$). (**E** and **F**) Anchorage-independent growth assay of the indicated stable cells. The quantitative analysis was shown adjacent to representative images (mean ± SD. n = 3. Student *t*-test. $^{**}p < 0.01$). (**G** and **H**) Annexin V-FITC apoptotic assays of the indicated stable cells treated with or without Cisplatin (DDP) for 48 h (10 μM). The quantitative analysis (mean ± SD. n = 3. Student *t*-test. $^{**}p < 0.01$) of apoptotic percentages of the indicated stable cells were shown as the histogram adjacent to representative flow cytometer images.

significantly decreased at the mRNA level in these HCC cells under hypoxia, whereas other YTH domain proteins remained unchanged or slightly reduced (Fig. 1B and Fig. S1). Consistently, the YTHDF2 protein level was also reduced under hypoxia in these HCC cells (Fig. 1C). To further confirm that hypoxia inhibits YTHDF2 expression, we used Cobalt(II) chloride ($CoCl_2$) which induces HIF1α expression in normoxia to mimic the effect of hypoxia. As expected, YTHDF2 was also remarkably declined under treatment of $CoCl_2$ in HCC cells (Fig. 1D). Moreover, the hypoxia-induced down-regulation of YTHDF2 was completely abolished by knocking down of HIF1α using siRNA in HCC cells (Figs. 1E and 1F), suggesting that the down-regulation of YTHDF2 by hypoxia is dependent on HIF1α in HCC cells. Taken together, our results show that YTHDF2 is specifically inhibited by hypoxia in HCC cells, implying YTHDF2 may be associated with HCC progression.

### *3.2. Overexpression of YTHDF2 suppresses HCC cell proliferation and growth in vitro and in vivo*

To explore the potential role of YTHDF2 in HCC, HEP3B, SMMC7721, QGY7703 and BEL7402 cells stably expressing Flag-tagged YTHDF2 were generated. Using different assays, we found that proliferation (Figs. 2A and 2B and Figs. S2A and S2B), colony formation (Figs. 2C and 2D and Figs. S2C and S2D) and anchorage-independent growth (Figs. 2E and 2F) were reduced while apoptosis induced by DDP

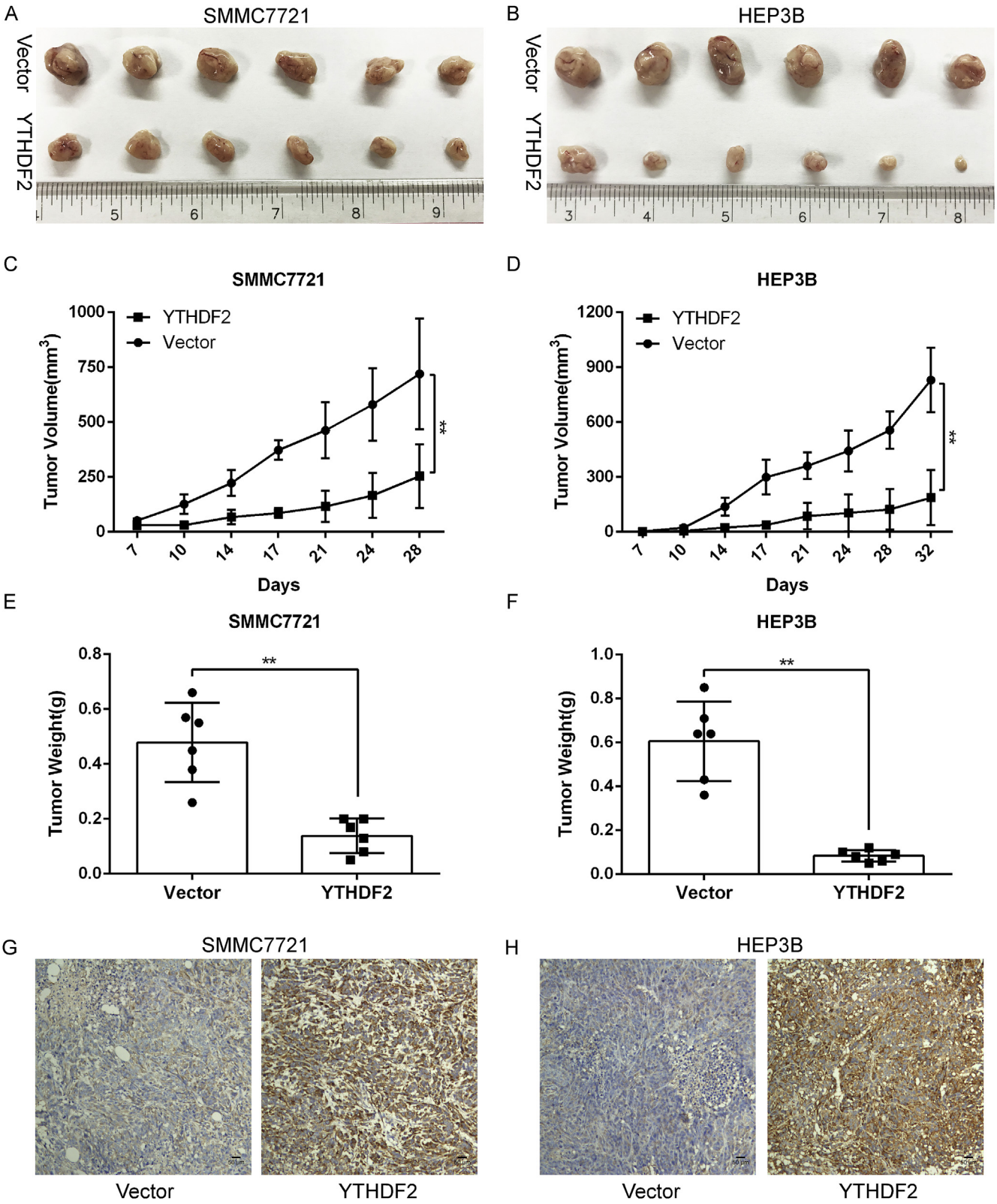


**Fig. 3.** YTHDF2 suppresses HCC growth in nude mice. (**A** and **B**) Nude mice were subcutaneously injected with the indicated stable cells, and tumors were dissected from nude mice after a month (n = 6). (**C** and **D**) Tumor growth in nude mice inoculated with the indicated stable cells was measured at the indicated time points (mean ± SD. n = 6. Student *t*-test. **p < 0.01). (**E** and **F**) Tumor weights of each group were shown as mean ± SD. n = 6. Student *t*-test. **$p < 0.01$. (**G** and **H**) Representative immunohistochemical staining of YTHDF2 from the xenograft tumors using the indicated stable cells.

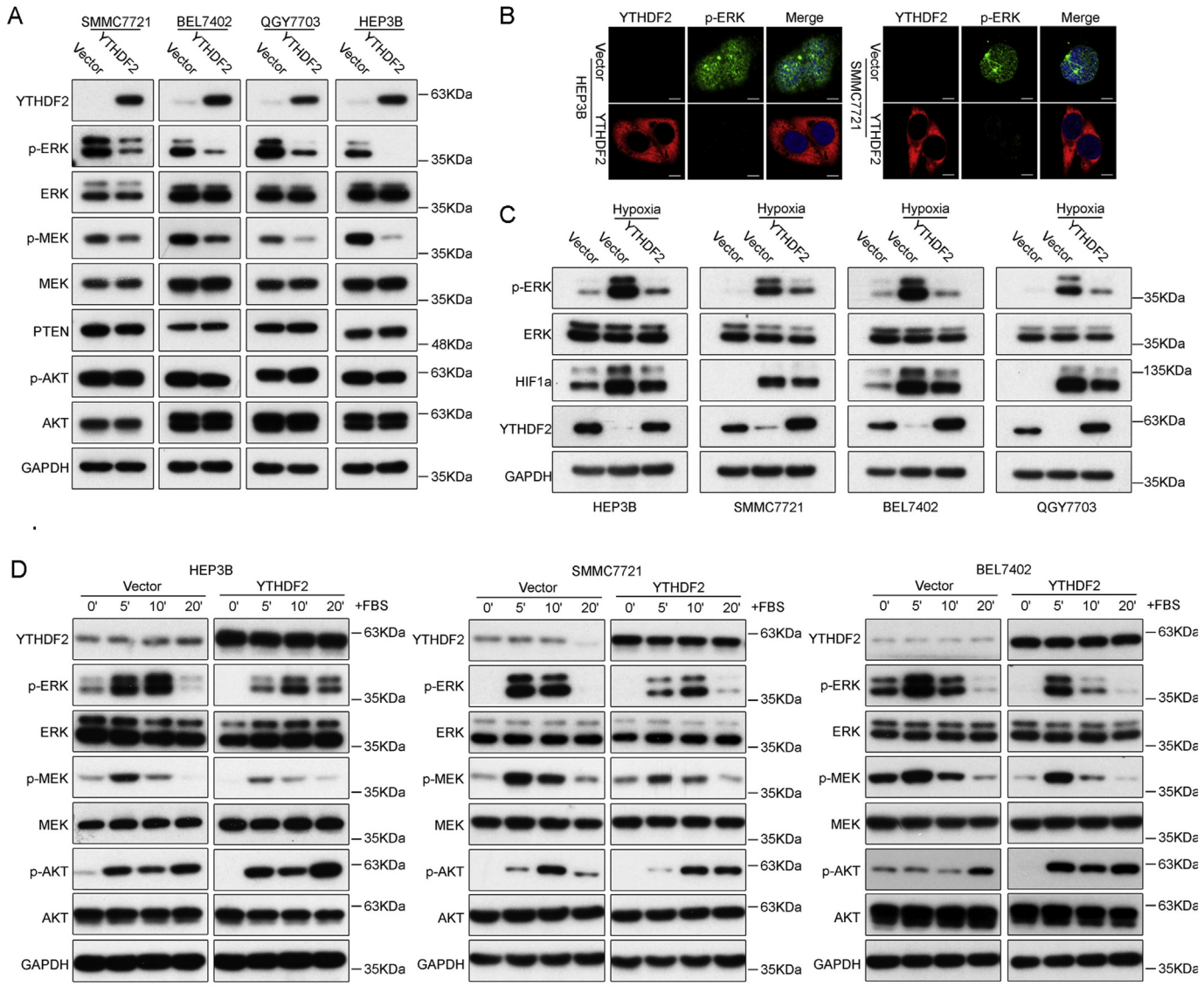


**Fig. 4.** YTHDF2 represses the MAPK/ERK pathway in HCC cells. (**A**) The indicated stable cells were lysed and analyzed by Western blotting. (**B**) The indicated stable cells were subjected to the immunofluorescence assay using anti-FLAG-YTHDF2 (red), anti-p-ERK (green) antibodies and DNA staining with Hoechst 33342. A merged view of three channels of the same filed was shown. Scale bar, 10 μm. (**C**) The indicated stable cells were exposed to 1% $O_2$ or 20% $O_2$ for 24 h, whole cell lysates were prepared and analyzed by Western blotting. (**D**) The indicated stable cells were cultured in serum-free DMEM for 24 h and stimulated with 10% FBS for the indicated periods, and then analyzed by western blotting.

was increased (Figs. 2G and 2H and Figs. S2E and S2F) in these cells stably expressing YTHDF2 compared to the cells carrying the vector only. Furthermore, as shown in Fig. 3 and Fig. S3, xenograft tumor burdens were significantly decreased in mice subcutaneously transplanted with HEP3B or SMMC7721 cells stably expressing YTHDF2 compared to those bearing the vector only. Collectively, our results suggest that YTHDF2 acts as a tumor suppressor in HCC.

On one hand, as shown in Fig. S4, neither cell proliferation nor colony-formation was affected when YTHDF2 was either knockdown or knockout by either two independent lenti-viral based short hairpin RNAs (shYTHDF2#1 and #2) or three highly efficient single-guided RNAs(sgYTHDF2#1, #2 and #3) in these HCC cells, suggesting that depletion of YTHDF2 alone is dispensable for the cell growth in HCC, and that the compensatory effect may present by other YTH domain proteins after depletion of YTHDF2 in HCC cells.

### 3.3. YTHDF2 inhibits ERK/MAPK signaling cascades in HCC cells

It is well known that both ERK/MAPK and PI3K/AKT signaling pathways are crucial in HCC proliferation and survival [21], we explored that whether overexpression of YTHDF2 impairs these two pathways in HCC cells. As shown in Fig. 4A and Fig. S5A, the phosphorylation of both ERK and MEK, but not of AKT, were obviously decreased in cells stably expressing YTHDF2 compared to the vector cells. Consistently, the nuclear accumulation of phosphorylated ERK was lower using immunofluorescent staining in cells stably expressing YTHDF2 compared to the vector cells (Fig. 4B and Fig. S5B). Moreover, the phosphorylation of ERK induced by hypoxia was also abrogated in cells stably expressing YTHDF2 (Fig. 4C), indicating that hypoxia may induce ERK phosphorylation by down-regulating YTHDF2 in HCC cells. Furthermore, as shown in Fig. 4D and Figs. S5C-S5F, the phosphorylation of both ERK and MEK, but not of AKT, induced by fetal bovine serum (FBS) or EGF at different time points were significantly impaired in cells stably expressing YTHDF2 compared to the vector cells. Taken together, our results suggest that overexpression of YTHDF2 suppresses cell proliferation through inhibiting the ERK/MAPK pathway rather than the PI3K-AKT pathway in HCC.

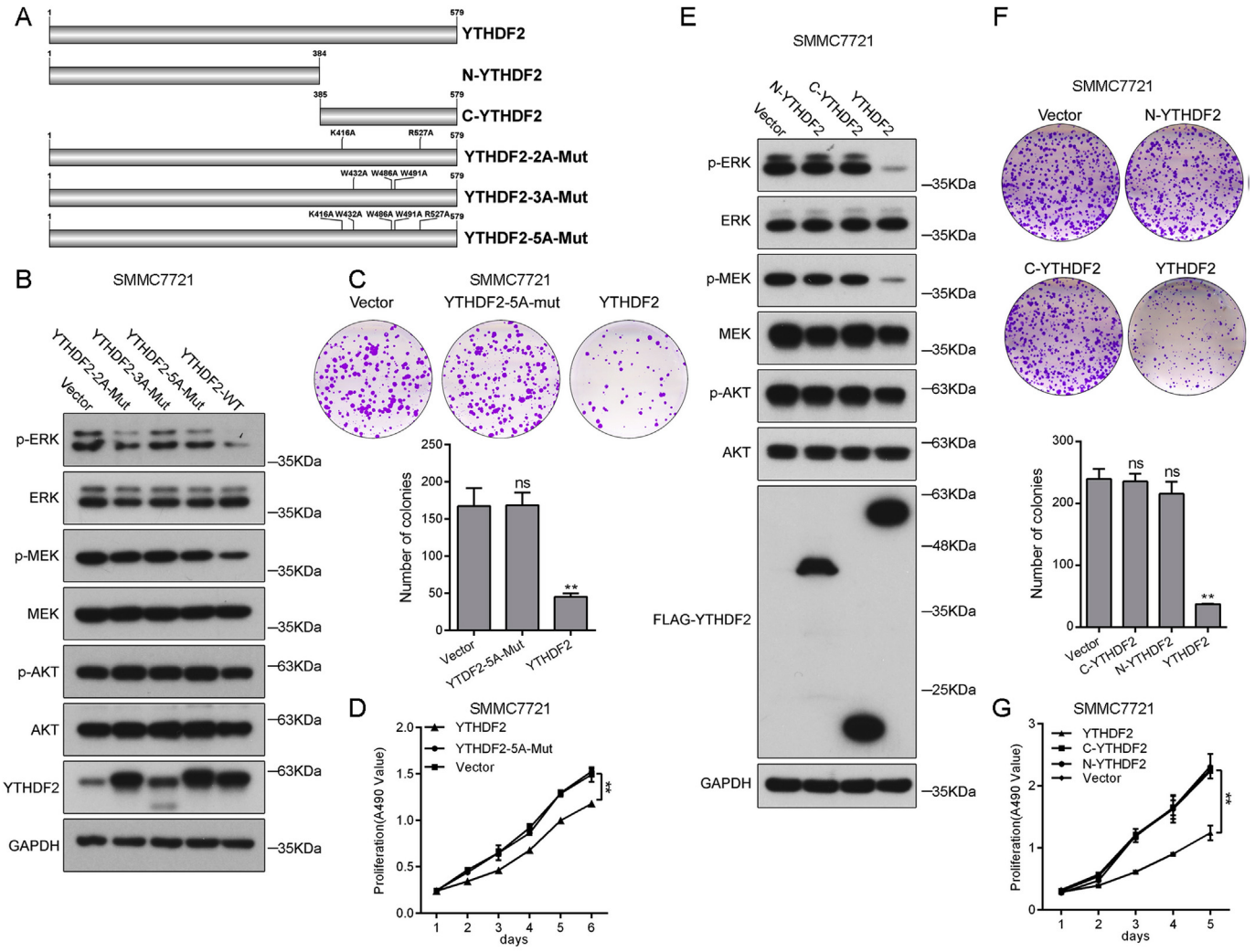


**Fig. 5.** Inhibition of YTHDF2 on the ERK/MAPK pathway and cell growth is dependent on its m6A recognition in HCC cells. (**A**) Schematic description of the YTHDF2 domains and point mutations. (**B**) The indicated stable SMMC7721 cells with YTHDF2 wild type (WT), YTHDF2-2A-Mut (K416A and R527A), YTHDF2-3A-Mut (W432A, W486A, W491A) and YTHDF2-5A-Mut (K416A, W432A, W486A, W491A and R527A) were analyzed by Western blotting. (**C**) Colony-formation assay of the indicated stable cells, and the quantitative analysis was shown below representative images (mean ± SD. n = 3. one way ANOVA with Bonferroni test. $^{**}p < 0.01$). (**D**) The cell viability of indicated stable cells were measured by MTT assay at different time points (mean ± SD. n = 3. one way ANOVA with Bonferroni test. $^{**}p < 0.01$. (**E**) SMMC7721 cells stably expressed Flag-N-domain YTHDF2 (N-YTHDF2), Flag-C-domain YTHDF2(C-YTHDF2), Flag-YTHDF2 (YTHDF2) and vector were analyzed by western blotting. (**F** and **G**) Colony-formation and MTT assays of indicated stable cells were analyzed as **C** and **D**.

### *3.4. YTHDF2 as the m$^6$A binding protein acts as a tumor suppressor in HCC*

It has been shown that YTHDF2 can regulate mRNA stability through both its N-domain, which localizes RNA to P-body, and its C-domain, which binds m$^6$A [3]. In addition, crystal structure of the YTH domain of YTHDF2 showed that K416/R527 are essential for binding of RNA backbone and that W432/W486/W491 contribute to the recognition of m$^6$A modification sites [14,15]. Therefore, series of truncations and mutations for YTHDF2 were constructed (Fig. 5A). As shown Figs. 5B and 5E and Figs. S6A and S6E, the decline of phosphorylation of ERK/MAPK induced by overexpression of YTHDF2 was not observed in cells stably expressing any of these YTHDF2 truncations or mutants. Likewise, the cell proliferation and colony formation were not altered in cells stably expressing the YTHDF2-5A mutant, N- or C-truncation (Figs. 5C, 5D, 5F, 5G and Figs. S6B-S6D and S6F-S6H). These results demonstrated that the loss of N-terminal domain or C-terminal domain and mutants of core amino acids in YTHDF2 completely abolished its inhibitory function in HCC cells, suggesting YTHDF2 acts as the m$^6$A binding protein to suppress cell proliferation and growth in HCC.

### *3.5. YTHDF2 suppresses ERK/MAPK signaling by destabilizing the EGFR mRNA in HCC*

To look into the potential targets for YTHDF2 in HCC cells, we focused on EGFR, IGF1R, MET, VEGFR and PDGFR, as they are upstream of the ERK/MAPK pathway and are mainly involved in HCC progression [22]. Among them, the EGFR mRNA level was the most significantly reduced in both HEP3B and SMMC7721 cells stably expressing YTHDF2 compared to the vector cells (Fig. 6A), and such a reduction was further confirmed at the protein level of EGFR using Western blotting (Fig. 6B) and immunofluorescent staining (Fig. 6C). Accordingly, as shown in Fig. 6D, the half-life of EGFR mRNA was significantly decreased in both SMMC7721 and HEP3B cells stably expressing YTHDF2 compared to the vector cells.

Next, we asked whether YTHDF2 directly binds the m$^6$A modification sites of EGFR mRNA. Using the pmirGlo dual-luciferase reporter fused with the 3'-UTR fragment of EGFR, the luciferase activity was significantly reduced in cells stably expressing YTHDF2 compared to the vector cells (Fig. 6E). Using the m$^6$AVar database [23] to search for potential m$^6$A modification sites (DRACH) in EGFR mRNA, high

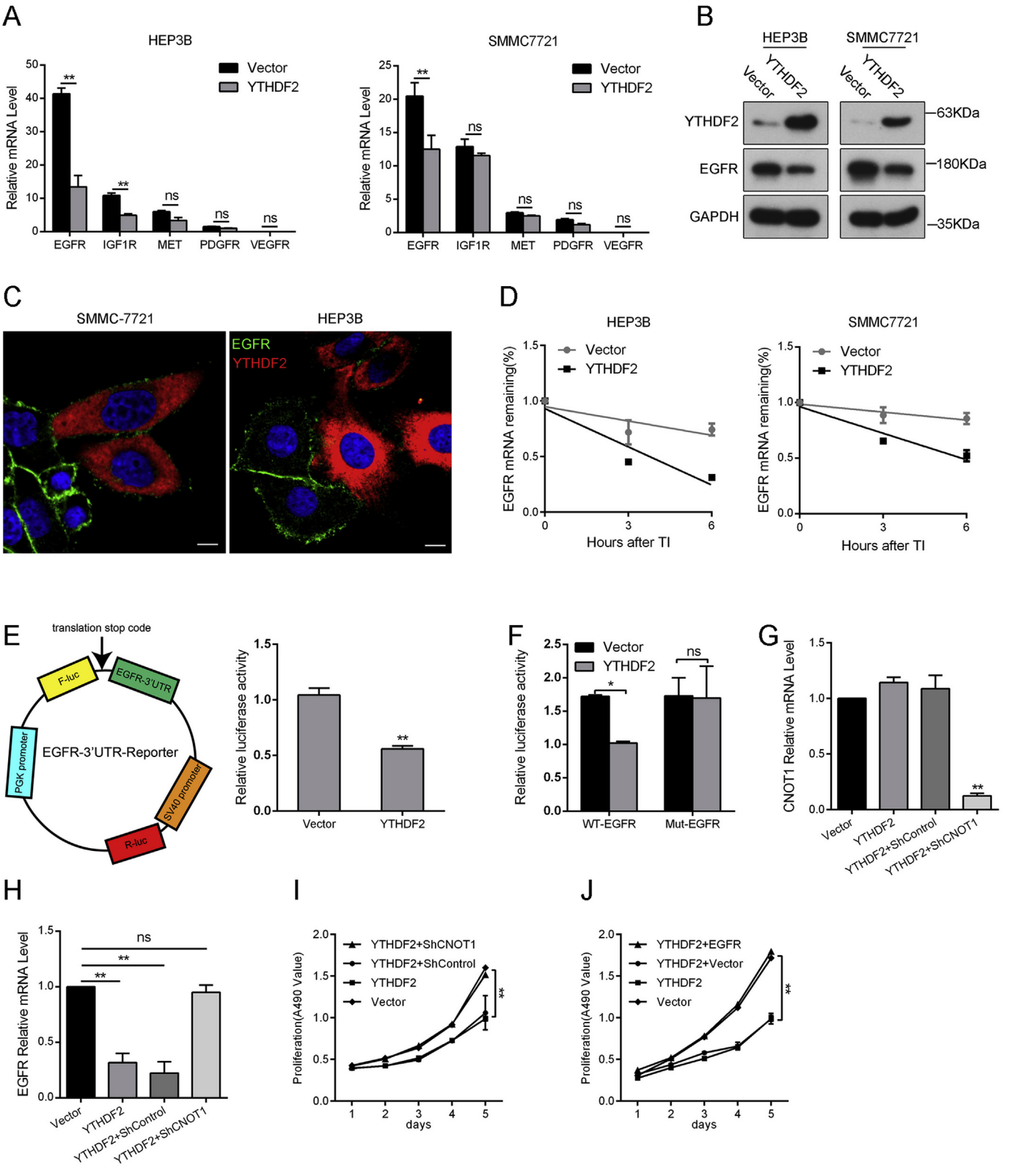


*(caption on next page)*

confidence m$^6$A motifs nearby stop codon in the 3'-UTR of EGFR was predicted, and the mutant of such motifs in the dual-luciferase reporter fused with the 3'-UTR of EGFR was generated. As shown in Fig. 6F, the reduction of luciferase activity in cells stably expressing YTHDF2 was abolished by such a mutant. Moreover, either knocking down of CNOT1 or ectopic expression of EGFR abrogated the inhibition of YTHDF2 on cell proliferation in cells stably expressing YTHDF2 (Figs. 6G–6J). Taken together, our results indicate that YTHDF2 acts as a tumor suppressor by directly binding the m$^6$A modification site of EGFR 3'-UTR to promote the degradation of EGFR mRNA in HCC cells.

**Fig. 6.** YTHDF2 inhibits cell proliferation and the ERK/MAPK pathway via accelerating the degradation of EGFR mRNA. (**A**) The mRNA levels of EGFR, IGF1R, MET, PDGFR and VEGFR from the indicated stable cells were evaluated by Quantitative RT-PCR (mean ± SD. n = 3. two way ANOVA with Bonferroni test. $^{**}p < 0.01$). (**B**) The indicated stable cells were analyzed by Western blotting, GPADH was used as the loading control (n = 3). (**C**) The indicated stable cells were fixed by 4% paraformaldehyde and subjected to immunofluorescence staining using both anti-Flag and anti-EGFR antibodies. DNA was stained with Hoechest 33342(n = 6). Scale bar, 10 μm. (**D**) The indicated stable cells were incubated with actinomycin D for 3 h and 6 h, and the half-life of EGFR mRNA was analyzed by quantitative RT-PCR and all values were normalized to HPRT (mean ± SD. n = 3). (**E**) SMMC7721 cells stably expressing YTHDF2 or vector were transfected with the indicated dual-luciferase reporters and relative luciferase activity was measured (mean ± SD. n = 3. Student *t*-test. $^{**}p < 0.01$). (**F**) SMMC7721 cells stably expressing YTHDF2 or vector were transfected with the indicated dual-luciferase reporter and relative luciferase activity was measured (mean ± SD. n = 3. two way ANOVA with Bonferroni test. $^{**}p < 0.01$). (G)SMMC7721 cells expressing YTHDF2 were stably transfected shRNA targeting CNOT1 or non-targeting control. CNOT1 mRNA level was determined by quantitative RT-PCR (mean ± SD. n = 3. one way ANOVA with Bonferroni test. $^{**}p < 0.01$). (H)EGFR mRNA level of indicated stable cells used in (G) was evaluated by quantitative RT-PCR (mean ± SD. n = 3. one way ANOVA with Bonferroni test. $^{**}p < 0.01$). (I) Cell viability of indicated stable cells used in (G) were measured by MTT assay (mean ± SD. n = 3. one way ANOVA with Bonferroni test. $^{**}p < 0.01$). (J) SMMC7721 cells expressing YTHDF2 were stably expressed EGFR or vector by lentivirus overexpression system and cell viability of indicated stable cells were assessed by MTT assay (mean ± SD. n = 3. one way ANOVA with Bonferroni test. $^{**}p < 0.01$).

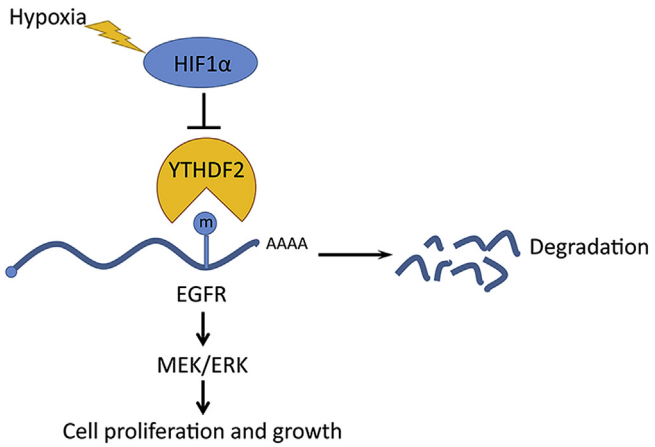


**Fig. 7.** The proposed model for function and mechanism of YTHDF2 in HCC. The YTHDF2, which was specifically down-regulated by hypoxia in HCC, may function as a tumor suppressor by negatively modulating the EGFR mRNA stability via binding the m$^6$A site in the EGFR 3'UTR of mRNA, which in turn impairs the MEK/ERK pathway and consequently impedes the cell proliferation and growth.

## 4. Discussion

In this report, we have demonstrated that YTHDF2 was specifically down-regulated by hypoxia in HCC cells, and that YTHDF2 may function as a tumor suppressor in HCC by negatively modulating the EGFR mRNA stability via its binding the m$^6$A site in the EGFR 3'UTR of mRNA, which in turn impairs the MEK/ERK pathway and consequently impedes the cell proliferation and growth, as illustrated in Fig. 7.

YTH domain proteins in mammalian can be divided into three categories, YTHDF family (YTHDF1, YTHDF2 and YTHDF3), YTHDC1 and YTHDC2 proteins, they share the YTH domain so that all of them can bind the m$^6$A sites in mRNA [24]. But their sizes and overall domain organization confer their different target mRNAs and functions. For instance, YTHDF1, YTHDF3 and YTHDC2 regulate translation efficiency of their target mRNAs [25–27], YTHDF2, YTHDF3 and YTHDC2 accelerate degradation of their target mRNAs [3,26,27], and YTHDC1 plays a critical role in mRNA splicing and nuclear export of N(6)-methyladenosine methylated mRNAs [28,29]. High expression of YTHDF1 is related to the poor prognosis in HCC and colorectal cancer [30,31] and YTHDC2 promotes metastasis in colon cancer [32]. Our results show that YTHDF2 may function as a tumor suppressor in HCC, as overexpression of YTHDF2 inhibits cell proliferation and growth, and promotes apoptosis in HCC cells (Fig. 2 and Fig. S2). Interestingly, Yang et al., has recently reported that YTHDF2 is closely associated with the malignancy of HCC, as the positive rate of YTHDF2 was 35.6% (67/188) in HCC tissues [33]. However, knockdown or knockout of YTHDF2 in HCC cells showed minimal effect on these events, suggesting that the compensatory effect may exist after depletion of YTHDF2 in HCC cells due to all YTH domain proteins share some similar target mRNAs [26]. It has previously reported that hypoxia can induce expression of ALKBH5 in breast cancer cells [12], and this induction of ALKBH5 by hypoxia was also observed in HCC cells (Fig. 1A). Intriguingly, the down-regulation of YTHDF2 by hypoxia was the most significant in HCC cells compared to the other YTH domain proteins, which were marginally altered by hypoxia (Fig. S1). In fact, hypoxia has already been reported to enhance of a subset of mRNA stability including VEGF (vascular endothelial growth factor), Glut1 (glucose transporter) and c-MYC through regulation of m$^6$A modification [34,35].

YTHDF2 is the core component of m$^6$A binding protein complex which regulates its target mRNA stability [3,16]. Here, we have identified the EGFR 3'-UTR mRNA as a direct downstream target of YTHDF2 in HCC cells (Fig. 6), and the inhibition of YTHDF2 on cell proliferation and growth is dependent on its destabilization of the EGFR mRNA in HCC cells. EGFR as a new target of YTHDF2 may explain why overexpression of YTHDF2 inhibited the MEK/ERK pathway to suppress cell proliferation and growth in HCC cells, EGFR is a main upstream of the ERK/MAPK pathway and is closely involved in HCC progression [38]. This finding may suggest that YTHDF2 as a m$^6$A binding protein may be specially associated with the HCC progression, which is desired to be further investigated in the future. On the other hand, other targets could not be excluded for the functions of YTHDF2 in the HCC progression. For instance, YTHDF2 displayed dual effects in the pancreatic cancer cells, YTHDF2 promoted cell proliferation by activating AKT signaling pathway and inhibited cell migration and invasion by destabilizing YAP mRNA [17]; YTHDF2 regulated stability of MYC mRNA to controls the response/sensitivity of leukemia cells to R-2HG [36]; Loss of YTHDF2 also promoted hematopoietic stem cells regeneration through stabilization of its key m6A-marked targets such as Tal1 [37]. Collectively, the multiple functions of YTHDF2 in cancers or diseases may depend on degradation of its target mRNAs.

## Conflicts of interest

We have no conflicts of interest to declare.

## Acknowledgements

This work was supported by and Science and Technology Program of Guangzhou, China (Grant No.201508020102 to T. K.); the National Key Research and Development Program of China [2016YFC0904601 and 2016YFA0500304 to T. K.], and the National Nature Science Foundation in China (NSFC) [81502512 to D. L., 8187111580 to H. M., 81530081 and 31571395 to T. K.].

## Appendix A. Supplementary data

Supplementary data to this article can be found online at https://doi.org/10.1016/j.canlet.2018.11.006.

## References


[1] L.A. Torre, F. Bray, R.L. Siegel, J. Ferlay, J. Lortet-Tieulent, A. Jemal, Global cancer statistics, 2012, CA A Cancer J. Clin. 65 (2015) 87–108.
[2] J.M. Llovet, J. Zucman-Rossi, E. Pikarsky, B. Sangro, M. Schwartz, M. Sherman, et al., Hepatocellular carcinoma, Nature Rev. Dis. Prim. 2 (2016) 16018.
[3] X. Wang, Z. Lu, A. Gomez, G.C. Hon, Y. Yue, D. Han, et al., N6-methyladenosine-dependent regulation of messenger RNA stability, Nature 505 (2014) 117–120.
[4] S. Lin, J. Choe, P. Du, R. Triboulet, R.I. Gregory, The m(6)A methyltransferase METTL3 promotes translation in human cancer cells, Mol. Cell 62 (2016) 335–345.
[5] B. Tan, H. Liu, S. Zhang, S.R. da Silva, L. Zhang, J. Meng, et al., Viral and cellular N (6)-methyladenosine and N(6),2'-O-dimethyladenosine epitranscriptomes in the KSHV life cycle, Nature Microbiol. 3 (2018) 108–120.
[6] B.S. Zhao, X. Wang, A.V. Beadell, Z. Lu, H. Shi, A. Kuuspalu, et al., m6A-dependent maternal mRNA clearance facilitates zebrafish maternal-to-zygotic transition, Nature 542 (2017) 475–478.
[7] X. Deng, R. Su, H. Weng, H. Huang, Z. Li, J. Chen, RNA N(6)-methyladenosine modification in cancers: current status and perspectives, Cell Res. 28 (2018) 507–517.
[8] H. Weng, H. Huang, H. Wu, X. Qin, B.S. Zhao, L. Dong, et al., METTL14 inhibits hematopoietic stem/progenitor differentiation and promotes leukemogenesis via mRNA m(6)A modification, Cell Stem Cell 22 (2018) 191–205 e9.
[9] C. Zhang, Y. Chen, B. Sun, L. Wang, Y. Yang, D. Ma, et al., m(6)A modulates haematopoietic stem and progenitor cell specification, Nature 549 (2017) 273–276.
[10] Z. Li, H. Weng, R. Su, X. Weng, Z. Zuo, C. Li, et al., FTO plays an oncogenic role in acute myeloid leukemia as a N6-methyladenosine RNA demethylase, Cancer Cell 31 (2017) 127–141.
[11] S. Zhang, B.S. Zhao, A. Zhou, K. Lin, S. Zheng, Z. Lu, et al., m6A demethylase ALKBH5 maintains tumorigenicity of glioblastoma stem-like cells by sustaining FOXM1 expression and cell proliferation Program, Cancer Cell 31 (2017) 591–606 e6.
[12] C. Zhang, D. Samanta, H. Lu, J.W. Bullen, H. Zhang, I. Chen, et al., Hypoxia induces the breast cancer stem cell phenotype by HIF-dependent and ALKBH5-mediated m (6)A-demethylation of NANOG mRNA, Proc. Natl. Acad. Sci. U.S.A. 113 (2016) E2047–E2056.
[13] K.D. Meyer, S.R. Jaffrey, Rethinking m(6)A readers, writers, and erasers, Annu. Rev. Cell Dev. Biol. 33 (2017) 319–342.
[14] F. Li, D. Zhao, J. Wu, Y. Shi, Structure of the YTH domain of human YTHDF2 in complex with an m(6)A mononucleotide reveals an aromatic cage for m(6)A recognition, Cell Res. 24 (2014) 1490–1492.
[15] T. Zhu, I.A. Roundtree, P. Wang, X. Wang, L. Wang, C. Sun, et al., Crystal structure of the YTH domain of YTHDF2 reveals mechanism for recognition of N6-methyladenosine, Cell Res. 24 (2014) 1493–1496.
[16] H. Du, Y. Zhao, J. He, Y. Zhang, H. Xi, M. Liu, et al., YTHDF2 destabilizes m(6)A-containing RNA through direct recruitment of the CCR4-NOT deadenylase complex, Nat. Commun. 7 (2016) 12626.
[17] J. Chen, Y. Sun, X. Xu, D. Wang, J. He, H. Zhou, et al., YTH domain family 2 orchestrates epithelial-mesenchymal transition/proliferation dichotomy in pancreatic cancer cells, Cell Cycle 16 (2017) 2259–2271.
[18] Y. Li, C.K. Tsang, S. Wang, X.X. Li, Y. Yang, L. Fu, et al., MAF1 suppresses AKT-mTOR signaling and liver cancer through activation of PTEN transcription, Hepatology 63 (2016) 1928–1942.
[19] C.Y. Chen, N. Ezzeddine, A.B. Shyu, Messenger RNA half-life measurements in mammalian cells, Methods Enzymol. 448 (2008) 335–357.
[20] L. Schito, G.L. Semenza, Hypoxia-inducible factors: master regulators of cancer progression, Trends Canc. 2 (2016) 758–770.
[21] S. Whittaker, R. Marais, A.X. Zhu, The role of signaling pathways in the development and treatment of hepatocellular carcinoma, Oncogene 29 (2010) 4989–5005.
[22] P.J. Roberts, C.J. Der, Targeting the Raf-MEK-ERK mitogen-activated protein kinase cascade for the treatment of cancer, Oncogene 26 (2007) 3291–3310.
[23] Y. Zheng, P. Nie, D. Peng, Z. He, M. Liu, Y. Xie, et al., m6Avar: a database of functional variants involved in m6A modification, Nucleic Acids Res. 46 (D1) (2017) D139–D145.
[24] D.P. Patil, B.F. Pickering, S.R. Jaffrey, Reading m(6)A in the transcriptome: m(6)a-binding proteins, Trends Cell Biol. 28 (2018) 113–127.
[25] X. Wang, B.S. Zhao, I.A. Roundtree, Z. Lu, D. Han, H. Ma, et al., N(6)-methyladenosine modulates messenger RNA translation efficiency, Cell 161 (2015) 1388–1399.
[26] H.L. Shi, X. Wang, Z.K. Lu, B.X.S. Zhao, H.H. Ma, P.J. Hsu, et al., YTHDF3 facilitates translation and decay of N-6-methyladenosine-modified RNA, Cell Res. 27 (2017) 315–328.
[27] P.J. Hsu, Y. Zhu, H. Ma, Y. Guo, X. Shi, Y. Liu, et al., Ythdc2 is an N(6)-methyladenosine binding protein that regulates mammalian spermatogenesis, Cell Res. 27 (2017) 1115–1127.
[28] I.A. Roundtree, G.Z. Luo, Z. Zhang, X. Wang, T. Zhou, Y. Cui, et al., YTHDC1 mediates nuclear export of N(6)-methyladenosine methylated mRNAs, eLife 6 (2017).
[29] W. Xiao, S. Adhikari, U. Dahal, Y.S. Chen, Y.J. Hao, B.F. Sun, et al., Nuclear m(6)A reader YTHDC1 regulates mRNA splicing, Mol. Cell 61 (2016) 507–519.
[30] X. Zhao, Y. Chen, Q. Mao, X. Jiang, W. Jiang, J. Chen, et al., Overexpression of YTHDF1 is associated with poor prognosis in patients with hepatocellular carcinoma, Cancer Biomark. : Sect. A Dis. Markers 21 (2018) 859–868.
[31] Y. Nishizawa, M. Konno, A. Asai, J. Koseki, K. Kawamoto, N. Miyoshi, et al., Oncogene c-Myc promotes epitranscriptome m(6)A reader YTHDF1 expression in colorectal cancer, Oncotarget 9 (2018) 7476–7486.
[32] A. Tanabe, K. Tanikawa, M. Tsunetomi, K. Takai, H. Ikeda, J. Konno, et al., RNA helicase YTHDC2 promotes cancer metastasis via the enhancement of the efficiency by which HIF-1alpha mRNA is translated, Cancer Lett. 376 (2016) 34–42.
[33] X. Duan, J. Hu, Y. Wang, J. Gao, D. Peng, L. Xia, MicroRNA-145: a promising biomarker for hepatocellular carcinoma (HCC), Gene 541 (2014) 67–68.
[34] N.J. Fry, B.A. Law, O.R. Ilkayeva, C.L. Holley, K.D. Mansfield, N(6)-methyladenosine is required for the hypoxic stabilization of specific mRNAs, RNA 23 (2017) 1444–1455.
[35] K.R. Carraway, E.M. Johnson, T.C. Kauffmann, N.J. Fry, K.D. Mansfield, Hypoxia and Hypoglycemia synergistically regulate mRNA stability, RNA Biol. 14 (2017) 938–951.
[36] R. Su, L. Dong, C. Li, S. Nachtergaele, M. Wunderlich, Y. Qing, et al., R-2HG exhibits anti-tumor activity by targeting FTO/m(6)A/MYC/CEBPA signaling, Cell 172 (2017) 90–105.
[37] Z. Li, P. Qian, W. Shao, H. Shi, X.C. He, M. Gogol, et al., Suppression of m(6)A reader Ythdf2 promotes hematopoietic stem cell expansion, Cell Res. 28 (2018) 904–917.
[38] K. Komposch, M. Sibilia, EGFR signaling in liver diseases, Int. J. Mol. Sci. 17 (2015).